Catalysis Science & Technology

PAPER

Deoxydehydration of glycerol in presence of rhenium compounds: reactivity and mechanistic aspects†

Cite this: DOI: 10.1039/c8cy02478b

Massimiliano Lupacchini,‡[a] Andrea Mascitti,‡[a] Valentino Canale,[b] Lucia Tonucci,[c] Evelina Colacino,[d] Maurizio Passacantando,[e] Alessandro Marrone *[b] and Nicola d'Alessandro *[a]

Allyl alcohol (AA) was obtained by the deoxydehydration (DODH) of glycerol performed in the presence of a number of Re compounds (oxides, phosphine and halide derivatives) in alcoholic solvent or in neat conditions. Independently on starting Re species, the resulting catalytic process featured a delay time, necessary to start the formation of both AA and an Re-alkoxide precipitate. However, no delay time was detected by operating DODH using a preformed precipitate obtained by either Re source. As a consequence, and based on IR spectral analysis, it was hypothesized that the Re precipitate is the actual catalyst of DODH. The mechanism of DODH catalysis operated by methyltrioxorhenium (MTO) was studied by experimental and theoretical approaches. The results suggest that MTO releases methane with the formation of an Re^{VII} alkoxide that subsequently aggregates by yielding the precipitate. The Re^{VII} centre precipitate surface then undergoes reduction by forming Re^{V} catalytic spots. The calculated kinetics also indicate that the detected latency can be ascribed to the presence of two high barriers, *i.e.* methane release and $Re^{VII} \rightarrow Re^{V}$ reduction, whereas the downstream processes, *i.e.* glycation and AA release, are not rate determining.

Received 7th December 2018,
Accepted 23rd April 2019

DOI: 10.1039/c8cy02478b

rsc.li/catalysis

Introduction

"*Historically, one relies on Mother Nature to provide all the material needs of society*". With this sentence, Li and Anastas well described the present and the future of green chemistry.[1] In this regard, among the twelve Green Chemistry Principles,[2] the seventh clearly pushes the use of renewable feedstocks both as potential energy vectors[3] and as starting materials for chemicals.[4] This strategy is even more valuable if many derivatives are commonly handled, as they have been until now, as waste. In this respect, the waste generated by industrial chains employing biomass could be supportive in reducing the world-wide dependence on fossil resources.

In the European Union alone, 700 million tonnes of biowaste are produced per year, causing both environmental and economic concerns.[5] Among the above-mentioned amount of biowaste, polyols quantitatively represent the most important group and so we can consider them as a natural source of a series of materials otherwise obtainable only from fossil resources. For example, low-polarity chemicals, typically obtainable mainly from fossil resources, can now be produced by a deoxygenation step from bio-based by-products.[6] Obviously, to be adopted, the transformation technologies must be particularly sustainable, employing green technologies and experimental conditions which are not very harsh.[7]

The deoxydehydration reaction (DODH) represents the most intriguing tool to obtain alkenes from natural polyols and, until now, the most promising and investigated catalysts for such reactions are rhenium-based[8] even if, in some recent reports, vanadium[9] and molybdenum[10] have shown promising activities (Scheme 1).[11]

The first DODH reaction reported in the literature was in 1996 where a high oxidation state rhenium species was used

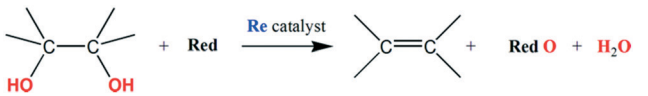

Scheme 1 DODH reaction pathway of a vicinal diol catalysed by rhenium compounds.

[a] *Department of Engineering and Geology, University "G. d'Annunzio" of Chieti-Pescara, Via dei Vestini, 31, I-66100, Chieti Scalo, Italy. E-mail: nicola.dalessandro@unich.it*
[b] *Department of Pharmacy, University "G. d'Annunzio" of Chieti-Pescara, Via dei Vestini, I-66100, Chieti Scalo, Italy*
[c] *Department of Philosophical, Educational and Economic Sciences, University "G. d'Annunzio" of Chieti-Pescara, Via dei Vestini, I-66100, Chieti Scalo, Italy*
[d] *Institut Charles Gerhardt de Montpellier (ICGM), UMR-5253 CNRS-UM-ENSCM, c/o Ecole Nationale Supérieure de Chimie de Montpellier, 8 Rue de l'Ecole Normale, 34296, Montpellier Cedex 05, France*
[e] *Department of Physical and Chemical Sciences, University of L'Aquila, Via Vetoio, I-67100 L'Aquila, Italy*

† Electronic supplementary information (ESI) available: dalessandro_DODH_CatSciTechnol.doc. See DOI: 10.1039/c8cy02478b

‡ These authors contributed equally.

as a catalyst.[12] However, despite the indisputable innovative value of this work, at that time – twenty years ago – several drawbacks were ascribed to the use of this material and some of them are still unsolved.

Undoubtedly, rhenium is a metal with a high affinity towards oxygenated organics. For example, oxygen transfer can be easily observed starting from either Re^{III} or Re^{V}.[13] By combining a reducing agent with rhenium derivatives, a desirable catalytic system to deoxygenate, above all, natural polyols is obtained.[14] Phosphine in a stoichiometric amount was the reductant used by Cook and Andrews,[12] but actually the use of a greener and cheaper alcohol that can sometimes be the reagent itself (*i.e.*, glycerol) is preferable.[15] The reaction medium is also important and good yields were often obtained in the past by employing apolar solvents like aromatics,[8a,d,12,16] although the current trend is to use common and cheap alcohols or, even better, to conduct the reaction without any solvent.[8b,15,17]

Among widely available natural polyols, glycerol represents an important example since it is formed in about 10% weight, from the transesterification of natural lipids. Crude glycerol has to be effectively utilized to contribute to the viability of biodiesel and it is more and more necessary to find new processes and new methodologies to convert glycerol into valuable fine chemicals using all the available pathways both chemical or biotechnological. Glycerol can serve as a feedstock for polymers,[18] ethanol,[19] hydrogen[20] and valuable alcohols like *n*-propanol[21] and *n*-butanol.[22]

In our research group, we undertook a research program on the valorisation of glycerol and recently we studied the rhenium oxide catalysed production of allyl alcohol (AA)[15] that could be considered in the future an important building-block to produce, for example, bioglycidol.[23]

Here, we will describe the same reaction but with a greater number of rhenium catalysts, involving oxides, halides and phosphines. Furthermore we believe that a suitable combination of experimental and theoretical data could help an understanding of the pending questions in the mechanism of the DODH reaction as, for example, discovering what are the metal oxidation states involved in the catalytic cycle.

Several reports have been published in the past,[24] but we maintain that the mechanism needs to be studied more deeply since, for example, not only Re^{VII} showed a satisfactory activity in the DODH. In particular, a density functional theory (DFT) study was focused on the glycerol DODH catalysed by methyltrioxorhenium (MTO) in terms of the evaluation of alternative pathways. The identification of active catalytic species and rate-limiting steps within the hypothesized DODH reaction pathways were the main outcomes of this theoretical investigation.

Experimental

Materials

Solvents and any other materials necessary for the experiments were used as received without any purification. Glycerol, AA, $ReOCl_3[S(CH_3)_2(OPPh_3)]$, ReI_3, $ReOCl_3(PPh_3)_2$, and NH_4ReO_4 were purchased from Sigma-Aldrich, while MTO, $ReCl_5$, $(PPh_3)_2ReO_2I$, Re_2O_7, $Re_2(CO)_{10}$, ReO_3 and Cp^*ReO_3 were purchased from Strem Chemical Inc.

Instruments

Nuclear magnetic resonance (NMR) spectra were recorded on a Bruker Avance DRX-300 spectrometer (7.05 Tesla) equipped with a high-resolution multinuclear probe operating in the range of 30–300 MHz. Spectra were recorded in an NMR tube (5 mm) that contained a closed co-axial capillary tube filled with 30 mM of 3-trimethylsilyl-2,2,3,3-tetradeutero propionic acid (sodium salt). Free induction decays were acquired at 22 °C using, for the proton, a pulse sequence (made by Bruker; zgcppr) that suppresses the water signal at 4.71 ppm. The spectral width was −1 to 12 ppm (3894.081 Hz) while a 90° excitation pulse, together with a 1 s relaxation delay, were used to collect 32 scans. Similarly ^{13}C spectra were acquired using again a suitable proton decoupling excitation pulse (zgdc; 90°) with 3 s of delay and a spectral width of 250 ppm (from −10 to 240 ppm).

The gas chromatography-mass spectrometer (GC-MS) equipment includes a Thermo Scientific Focus series gas chromatograph coupled to an ISQ mass-selective detector equipped with a split/splitless injection system (injections made in the split mode) and a low-polar HP-5 MS (cross-linked 5% phenyl methyl siloxane) capillary 30 m in length, 0.25 mm in diameter and with 0.25 μm film thickness, using high-purity helium as the carrier gas at a constant pressure of 30 kPa.

For the headspace analysis, the sample was thermostated at 45 °C for 5 min, after which 200 μL of aerial top layer solution was injected into the GC apparatus using a gas-tight syringe at a 5 : 1 split ratio.

The electron impact (EI) ion source was held at 250 °C, with a filament bias of 70 eV, transfer line at 250 °C, mass EI range 33–350 a, injector temperature of 250 °C, initial temperature of the analyses 38 °C (1 min), then 10 °C min^{-1} up to 250 °C (kept for 1 min), for a total acquisition time of 26 min.

Gas chromatographic analyses (GC) were performed using a Hewlett–Packard 6890 Series gas chromatograph system equipped with an FID, using a 30 m HP-5 capillary column (cross-linked 5% PH ME siloxane, 0.32 mm in diameter; 0.25 μm film thickness) with the injection port kept at 250 °C (carrier gas: high-purity helium with a pressure at the head of the column of 35 kPa). For the water solution, 0.5 μL was injected while for headspace analysis, the sample was thermostated at 45 °C for 5 min, after which 200 μL of aerial top layer solution was injected using a gas-tight syringe at a 5 : 1 split ratio.

The temperature programs were as follows: start at 60 °C with a hold time of 2 min, firstly increased at a rate of 5 °C min^{-1} to 130 °C (holding time 0 min) and then increased at a rate of 20 °C min^{-1} to 230 °C with a holding time of 2 min.

The UV-vis spectra were recorded using a Jenway 6505 system. Spectra were recorded in a 3 mL high-precision quartz

cell (made of Suprasil® quartz; Hellma), and the wavelength range was 200 nm to 600 nm.

Infrared spectra were measured on a Varian Scimitar 1000 FT-IR spectrometer with Cooled DTGS detector and Varian Resolutions 4.0 software. The samples were prepared on KBr pellets (1 mg in 100 mg of KBr).

DODH reaction procedure

In a 10 mL round glass vessel equipped with a magnetic stirrer and a rubber septum, 4 mL of 2,4-dimethyl-3-pentanol (DMP) and 0.05 (or 0.1) mmol of metal catalyst (11.1 or 22.2 mM) were initially added; subsequently, after the complete dissolution of the catalyst, 5 mmol (0.460 g; 1.11 M) of glycerol were added to the solution. The reaction mixture was heated to the desired temperature (140 °C) in a thermostatic oil bath and continuously purged with air or hydrogen (≈1 bubbles per second). The vessel was connected to a cold-water trap (25 mL, around 0 °C) by a steel double-pointed needle. The aqueous solution in the trap was sampled at the desired reaction time (200 μL each time) for the NMR spectra and for the GC analyses.

Preparation procedure of modified catalysts

In the same apparatus used for the DODH reactions, 4 mL of DMP and 0.05 mmol of metal catalyst (**1**, **2**, **4**, **5**, **7** and **11**; see Scheme 2) were added. The mixture was heated to 140 °C and kept at this temperature for a duration equal to the delay time detected for each Re derivative (Fig. 1). Then, after the removal of the reflux apparatus, the temperature was increased to 170 °C, facilitating the evaporation of DMP. After cooling the reaction mixture to room temperature, the residue was collected with chloroform and filtered on paper, recovering the solid that was then either used as the catalyst in the DODH experiments or employed for the IR spectroscopy characterisation.

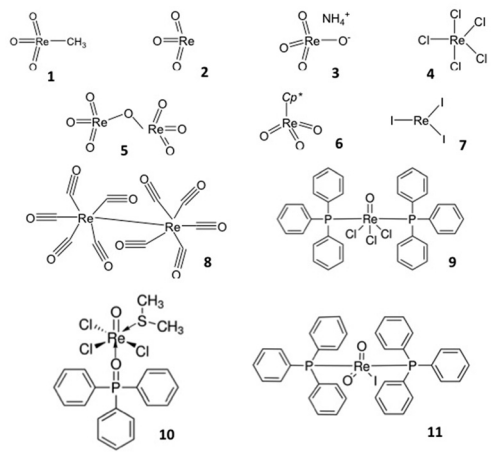

Scheme 2 Rhenium catalysts used in the DODH reaction of glycerol to give AA. Legend: **1**, methyltrioxorhenium (MTO); **2**, trioxorhenium; **3**, ammonium perrhenate; **4**, rhenium pentachloride; **5**, hepta-oxo-dirhenium; **6**, 1,2,3,4,5-pentamethylcyclopentadienyltrioxorhenium; **7**, rhenium triiodide; **8**, dirheniumdecacarbonyl; **9**, oxo-trichlorobis-(triphenylphosphine)rhenium; **10**, oxotrichloro[(dimethylsulfide)-triphenyl-phosphine oxide]rhenium; **11**, iododioxobis(triphenylphosphine)rhenium.

ICP AES measurements

Residual catalyst samples for elemental analyses and for ICP AES measurements were obtained as follow: in a 25 mL round glass vessel equipped with a magnetic stirrer and a rubber septum, 8 mL of DMP and 0.2 mmol of metal catalyst (0.1 for **5**) were added. The reaction mixtures were heated to 140 °C in a thermostatic oil bath for 8 hours. Then, after the removal of the reflux apparatus, the temperature was increased to 170 °C, facilitating the evaporation of DMP. After cooling the reaction mixture to room temperature, the residue was treated as explained below. Two parallel preparations were made for each Re catalyst used (**1**, **2**, **4**, **5**, **7** and **11**; see Scheme 2). One set of preparations was addressed to the ICP AES analyses, by simply treating each one with *aqua regia* and submitting the resulting acidic solution to a microwave-assisted mineralization procedure. The eluates were then collected in 10 mL volumetric flasks by ultrapure water and then analyzed by an ICP AES type Varian 720-ES Series. Calibration curves in the 0.1–100 μg L^{-1} range were prepared from Re standard solution (10 mg L^{-1}, ICP-MS grade, Carlo Erba Reagenti) in 2% HNO_3 (v/v). The remaining six samples were weighed, washed with chloroform first and then with water, and then heated in a muffle furnace at 450 °C under aerobic conditions for 4 hours. The resulting samples were again weighed and the Re content inside the catalyst samples was expressed, considering only the inorganic fraction of the residue, *i.e.* calculated as the whole mass of the sample – the weight loss at 450 °C.

XPS measurements

The chemical state of the different elements of the samples was analysed by using an X-ray photoelectron spectroscopy

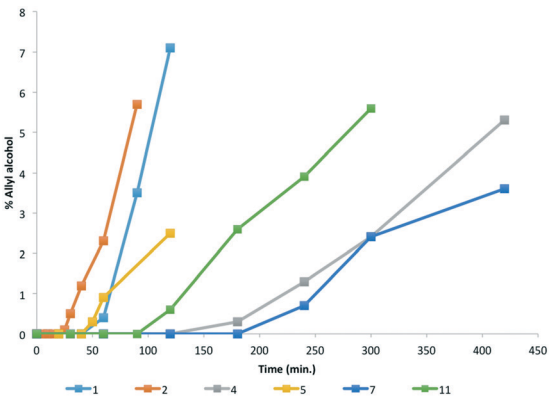

Fig. 1 Time courses relative to compounds **1** (light blue), **2** (orange), **4** (grey), **5** (yellow), **7** (blue) and **11** (green) at the beginning of the reaction. Note the delay times are different for each one (**1** = 45 min; **2** = 25 min; **4** = 120 min; **5** = 40 min; **7** = 180 min; **11** = 90 min). Reactions were conducted in an air atmosphere in DMP with 12.5 mM of each catalyst and 1.25 M of glycerol.

(XPS) system (PHI 1257), equipped with a hemispherical analyser. The X-rays were generated by a non-monochromatized Mg source ($h\nu$ = 1253.6 eV), and the measurements were taken in an ultrahigh vacuum at about 1×10^{-9} mm Hg. The binding energy (BE) calibration of the spectra was referred to the C 1s core level peak, located at BE = 284.8 eV. The analysis of the XPS core level peak data was performed by a fitting procedure and a Shirley function was used to consider the background. All the elements revealed for the different samples were acquired with a pass energy of 23 eV.

DFT methods

All calculations were performed using the Gaussian 09 program package.[25] The local minimum geometry of each Re^{VII} or Re^{V} species (see below) was calculated with the hybrid exchange–correlation functional B3LYP[26] and the following basis sets scheme: the basis set assigned by the LANL2DZ keyword describes the valence shell electrons of Re with a double-ζ plus one l + 1 polarization basis set[27] and uses a pseudopotential[28] to take into account relativistic effects affecting the core electrons; the all-electron 6-31G* by Pople[29] was employed to treat the remaining atoms; we hereafter denote this basis set scheme sbs (small basis set). Vibrational frequencies analyses were performed at the same level of theory (IEPCM/B3LYP/sbs) to confirm the correct nature of the optimized stationary points and to calculate zero-point energy and thermal corrections (under the hypothesis of ideal gas behaviour) for enthalpy and free energy estimations. Theoretical vibrational spectra were also calculated for Re^{VII} and Re^{V} dimer species (see below) by the scaling the calculated frequencies by a constant factor of 0.961.[30] The electronic energy of each B3LYP/sbs geometry was recalculated using a larger basis set scheme: i) the all-electron triple-ζ 6-311G+(d, p) basis set including one l + 1 polarization plus one s diffusion function for C, O, and H;[29c] ii) the Stuttgart relativistic small core potential[31] and the valence basis set[32] augmented with two f-type and one g-type polarization functions [$\zeta(f)$ = 0.327, 0.955; $\zeta(g)$ = 0.636][33] for Re. We hereafter denote this basis set scheme lbs (large basis set). The polarizable continuum model using the integral equation formalism variant (IEFPCM) implemented in Gaussian 09 (ref. 34) was then used to correct the gas phase free energy by the effect of a 2-propanol bulk (dielectric constant of 14.3).

Results

Rhenium-catalysed DODH of glycerol was carried out under aerobic (air flux) conditions or in the presence of an H_2 stream, always at 140 °C. Recovery of the reaction products was achieved using an ice-cooled water trap by collecting the gas flow coming from the reaction vessel, through which air or H_2 were continuously bubbled (ESI† Fig. S1).

The AA yields were referred to those measured at the end of the reaction regardless of the required times (ESI† in Fig. S2 a typical NMR spectrum of AA inside the water trap is reported). The catalyst was present in amounts ranging from 1 to 2% and the solvent was either a sacrificial alcohol (2,4-dimethyl-3-pentanol, DMP) or glycerol itself. The gas current was necessary to remove AA instantaneously and to convey it through a needle inside the cold trap containing water. Even if reactions were also operated in solvents like 3-octanol, 1,3-propandiol or 1-hexanol (with comparable product yields or lower), DMP was selected as the reference solvent for several reasons: i) its boiling point is high enough to allow it to operate the DODH reaction at reflux at high temperature (140 °C); ii) DMP oxidized competitively, thus preventing the side consumption of glycerol, and iii) secondary alcohols often appear more efficient for the majority of DODH reactions reported in the literature.[8d,17,35] As regards the mechanistic role of molecular hydrogen, we would like to recall previously reported experiments with deuterium gas that ruled out any participation of H_2 in the reduction step of glycerol, as demonstrated by the absence of deuterium in the reaction product, namely AA.[15]

Here, several rhenium complexes were tested as catalysts for the DODH of glycerol (Scheme 2). Together with those already considered in our previous publication,[15] which were mainly high-valence oxo-Re-species (**1**, **2**, **3** and **6**) and the inactive **8**, another six Re compounds were also selected to keep under consideration, above all, substituents other than oxygen, *i.e.* halogens (such as **4**, **9**, **10** and **11**) or phosphorus (*e.g.* **9**, **10** and **11**) or selecting some other low-valence-Re-species like **4** and **7**.

With the exception only of the inactive **8**, all tested Re compounds showed from moderate (5%; **3**) to high (≈90%; **1**, **2**, **11**) catalytic activity (Table 1).

While in neat glycerol the maximum theoretical product yield is only 50% (the other 50% of the glycerol acting as a reductant agent), the production of AA appears always more efficient in terms of yields and reaction times when reactions are conducted in DMP.

Also, H_2 noticeably increases product yields by an extent that depends on the nature of the rhenium catalyst, with its mechanistic role more likely to be ascribable to off-pathway prevention rather than to direct participation in the catalysis. The catalytic efficiency of phosphine derivatives is heavily enhanced by the presence of H_2 either neat or in DMP (doubled yields or more in an H_2 current), while rhenium oxides are less influenced by showing product yield increments ranging from 10 to 30% (Table 1).

Besides the above-mentioned reactivity framework, attention was focused on the phenomena observed during the course of the reactions. We always noted a delay time necessary for the initial production of AA. At the beginning of the reaction, and before AA starts to be formed, the alcoholic rhenium solution appeared colourless and homogeneous. In the course of reaction, the rhenium solution changed aspect both in colour, by turning yellow and then dark, and in its physical phase through a tendency to form a precipitate. These reaction features are shared by all the tested rhenium

Table 1 AA yields with rhenium catalysts, in aerobic (air) or H_2 atmosphere, at 140 °C and in neat glycerol or in DMP as solvent

Catalyst (mol%)	Exp. cond.	Yields, mol% (time, min)	
		Air	H_2
1 (2%)	Neat	14 (1320)	32 (500)
	DMP	61 (1200)	87 (1200)
2 (2%)	Neat	32 (1275)	34 (1005)
	DMP	64 (1800)	91 (800)
3 (2%)	Neat	0 (480)	0 (480)
	DMP	5 (1200)	7 (1200)
4 (1%)	Neat	5 (480)	11 (480)
	DMP	17 (1200)	38 (1200)
5 (1%)	Neat	28 (1440)	33 (1440)
	DMP	52 (1200)	68 (1200)
6 (2%)	Neat	0 (480)	0 (480)
	DMP	11 (1800)	15 (1320)
7 (1%)	Neat	16 (1440)	16 (1440)
	DMP	31 (1440)	60 (1380)
8 (2%)	Neat	0 (480)	0 (480)
	DMP	0 (480)	0 (480)
9 (1%)	Neat	11 (1440)	25 (1440)
	DMP	32 (1320)	81 (1230)
10 (1%)	Neat	13 (1440)	35 (1440)
	DMP	35 (1320)	80 (1320)
11 (1%)	Neat	16 (1440)	33 (1440)
	DMP	45 (1480)	84 (1200)

derivatives, even if the corresponding delay times are characterized by different extensions.

To gain more detailed information about the role played by the metal, compounds **1**, **2**, **4**, **5**, **7** and **11** underwent treatment at 140 °C, under the same experimental conditions used for the DODH in DMP, but sampling the presence of AA over very short time intervals. The delay times, relative to each employed Re compound, were extrapolated from the time course reported in Fig. 1, by scoring the time of initial AA detection.

Subsequently, analogous DODH experiments were carried out by employing modified catalysts obtained from **1**, **2**, **4**, **5**, **7** and **11** by treating each compound at 140 °C in DMP for the duration of the respective delay times (for the preparative procedure regarding these modified catalysts, see the experimental section). As a result, we noted that AA was formed almost immediately for all the tested catalysts, thus confirming the importance of different delay times for each starting rhenium compound.

Due to the important role played by the modifications occurring during the delay time in all the rhenium compounds, all the thermally modified derivatives were characterised by IR spectroscopy. The comparison of all IR spectra evidenced a significant overlap in spite of the differently processed catalysts (for the IR spectra, see the ESI† Fig. S3–S13). To better describe this outcome, the IR spectra of the precipitates formed by **1**, **4**, **5**, and **7** were reported in the same plot (Fig. 2).

Similarities were found mostly in three regions of the vibrational spectrum. Intense and broad signals were detected in the 1800–3500 cm^{-1} range and plausibly ascribed to C–H and O–H stretching. A group of multiple signals was detected in the 1000–1750 cm^{-1} range where C–O stretching and either C–C–H or C–O–H bending are located. The most intense signal was found in the 500–1000 cm^{-1} range, precisely around 920 cm^{-1} and this can be easily assigned to the stretching of Re═O. Also in this range, a less intense band around 700 cm^{-1} could be assigned either to the out-of-plane bending of O–H bonds or to the stretching of Re–O–Re oxo-bridges.

Comparing the spectra before and after the thermal treatment it is worth noting that, for all the rhenium derivatives taken into consideration, the signals dramatically changed after thermal treatment. To further support the transformation of rhenium derivatives before catalysing the reaction, we carried out a test on glycerol using monodeuterated DMP(-OD) and **1** as catalysts: the production of monodeuterated methane occurred only at the beginning of the reaction, as confirmed by GC-MS analyses (ESI† Fig. S14).

Treated rhenium residues, *i.e.* the precipitate obtained by the treatment of the catalyst under DODH conditions, were recovered and then re-used for DODH reactions by adding fresh glycerol. Interestingly, in this case, no delay time was needed and AA began to be formed as soon as the reaction media reached the required 140 °C (ESI† Fig. S15). On the other hand, when the precipitate was recovered at the end of the reaction, that is when the formation of AA stopped (after around 35–45% of yield in neat glycerol or after 80–90% of yield in DMP, also depending on the gas current employed), its reuse did not show any catalytic activity.

To get data responsive to the rhenium content in the catalyst, the amount of organic material present inside the residue, obtained through the evaporation of the solvent, was evaluated. Taking into account the samples obtained after 8 hours of treatment, two parallel sets of experiments were carried out, aiming to obtain samples both for ICP AES analyses and those necessary for the evaluation of the non-volatile organic matter adsorbed on the Re-residue (from the thermal

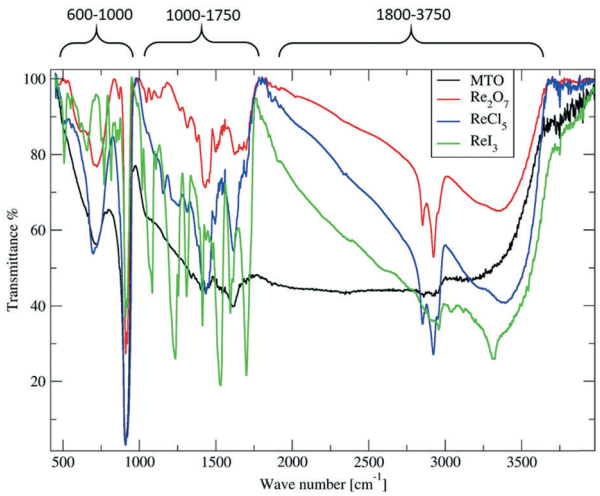

Fig. 2 IR spectra of the solids obtained by operating **1**, **4**, **5**, and **7**, *i.e.* MTO, Re_2O_7, $ReCl_5$, and ReI_3, respectively, under DODH conditions and after a delay time. All spectra were rescaled by assuming 100% of transmittance at 4000 cm^{-1}.

treatment at 450 °C). In the latter, the high temperature of the treatment transformed all the organic carbon to CO_2 and so only the rhenium derivatives remained. By subtracting the organic fraction from the rhenium residue, quantitative data for the metal ranging from 80 to 86% were obtained, while the remaining part of the residue seemed to be oxygen (with no presence of other elements like halogens). This means that the ratio between metal and oxygen ranges from 1/2 to 1/3. Analogous Re/O ratios were obtained by ICP AES experiments (see ESI† Tables S3 and S4).

As additional data some DODH reactions using a DMP–glycerol solution were performed, using an aliquot of the rhenium derivatives obtained after the thermal treatment at 450 °C. The AA yields were superimposable on those obtained through experiments carried out in the same manner but in the presence of modified catalysts (by treatment at 140 °C in the presence of DMP and in the absence of glycerol). In both cases, AA production started after a few minutes.

In order to characterise the Re surface valence chemistry, both XRD and XPS studies were carried out on different samples (**1**, and **1** after muffle treatment, **4**, **5** and **7**; see Scheme 2). XRD showed the amorphous character of the samples recovered after the DODH reactions (see ESI† Fig. S16). XPS survey scans, acquired in the range 0–1100 eV, revealed the presence of all the elements relative to the different prepared samples. No contaminant species were detectable within the sensitivity of the technique.

Fig. 3 shows the deconvoluted Re 4f electron core-level XPS spectra acquired from the different samples. The 4f level is formed by a double peak due to $4f_{7/2}$ and $4f_{5/2}$ levels, with a spin–orbit splitting of 2.4 eV. In Fig. 3, two vertical dashed lines located at BE values of 46.4 and 44.3 eV indicate the peak position of Re $4f_{7/2}$ for the Re^{VII} and $Re^{V/IV}$ species, respectively. Therefore, the most intense peak of the Re 4f raw data, corresponding to a BE of about 46 eV, was considered to be the sum of the Re $4f_{7/2}$ peaks for the Re^{VII} species and the Re $4f_{5/2}$ peaks for the $Re^{V/IV}$ species.[36] From these results a clear reduction of Re is evident due to the presence of the valence of 5+/4+. In addition, sample 7 also showed the presence of residual Re–I bonds (at a BE of 42.3 eV) and the presence of I 3d core level (at a BE of about 49 eV) (Fig. 3).

Because of the paramount importance of MTO in catalysis, further investigations were carried to shed more light on the DODH of glycerol catalysed by **1**.

The above described experimental outcomes are almost consistent with evidence from Hermann *et al.* for the formation of methyl-deficient polymetalates by either photochemical or thermal treatment of aqueous MTO.[37] However, in our hands the IR analyses indicated that alcohol moieties participate in the assembly of Re-based precipitates, suggesting that methyl group loss is probably paralleled by the metal coordination of alcohol. Indeed, as also reported by Nicholas *et al.*, alcohol coordination seems to be necessary to trigger the reduction of the Re centre, which is also a prerequisite for the catalysis of DODH.[38]

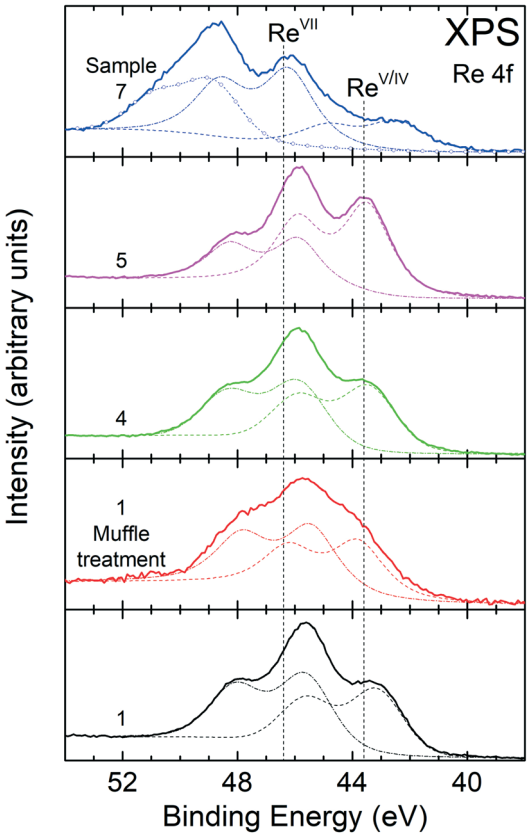

Fig. 3 XPS survey of the Re 4f region of the indicated samples (**1**, **1** after muffle treatment, **4**, **5** and **7**). The fitting curves are also included.

Computational studies were performed to investigate viable routes for this process by taking into account the experimental outcomes reported here. In particular, the theoretical investigation was addressed to five guiding pieces of evidence: 1) methane is released by operating the reaction with **1**; 2) re-catalysis always features a definite delay time; 3) methane release occurs during the delay time; 4) separation of a solid phase occurs in parallel with the methane release; 5) the precipitate recovered straight after the delay time efficiently catalyses the DODH of glycerol.

DFT calculations were firstly focused on possible mechanisms for the release of methane from **1** in the presence of secondary alcohol and further reduction of the yielded Re^{VII} species to the corresponding Re^{V} form. 2-Propanol (2-PrOH) was selected as a reduced model of DMP expected to disclose essentially the same reactivity but allowing a decrease in computational burden. Calculations indicate that the substitution of CH_3^- with 2-propanol alkoxide (2-PrO$^-$) on the Re centre leading to methane release is thermodynamically feasible with a reaction free energy of −18.5 kcal mol^{-1}. The results indicated that this process occurs with a concerted mechanism (ESI† Scheme S1) in which 2-PrOH coordinates on the Re centre by donating a proton to the leaving CH_3^-, as shown by the corresponding transition state structure (ESI† Fig. S17). The concerted proton shift and release of methane could be assisted by the active participation of the alcoholic

solvent through the formation of H-bond clusters chaining the oxygen of the entering 2-propanol to the carbon on the released methane. However, the bulky size of the solvent molecules is expected to disfavour the formation of these H-bond clusters close to the metal centre, but close enough to activate the attack on Re–C bond. For this reason, the use of continuum solvation was reputed to be reliable to model the bulk effects of solvation in the considered process.

Methane release leads to the formation of ReO_3(2-PrO) which is thus the rhenium species obtained under operating conditions that could actually initiate the formation of catalytically active species. We hypothesized that Re^{VII} alkoxide assembly occurs and that catalytic centres are consequently formed on the surface of the precipitate. To a first approximation, ReO_3(2-PrO) was assumed to model Re^{VII} pre-catalytic metal centres featuring the precipitate surface; in turn, they can undergo reduction by yielding Re^{V} catalytic centres, modelled by ReO_2(2-PrO). Such a proposed catalytic route is hereafter denoted as path B (Scheme 3).

The kinetic barrier calculated for the methane release process is 36.9 kcal mol^{-1}, and, although quite high, is expected to be overcome at high temperature. The Re^{VII} → Re^{V} conversion leading to ReO_2(2-PrO) with the release of acetone and water turned out to be slightly exergonic by −1 kcal mol^{-1}, and characterized by a high activation free energy of 40.3 kcal mol^{-1} (Scheme 4). The transition state structure for the Re^{VII} → Re^{V} conversion is also reported (Fig. 4, left).

To further corroborate the viability of path B, the thermodynamics and kinetics of MTO reduction *via* path A, consistent with MTO catalysis schemes often reported in the literature,[24,39] were also investigated. The direct reduction of **1** to the corresponding Re^{V} species turned out to be both thermodynamically and kinetically less favourable than methane release. In particular, it was found that the 2-PrOH coordination on **1**, representing the first step in path A, is endergonic by 21.4 kcal mol^{-1}, with a barrier of 38 kcal mol^{-1} for the subsequent reduction, thus leading to an overall energy barrier of 59.4 kcal mol^{-1} (Scheme 4). Therefore, the chemical processes downstream to reduction *via* path B are all thermodynamically favoured and affected by very low kinetic barriers

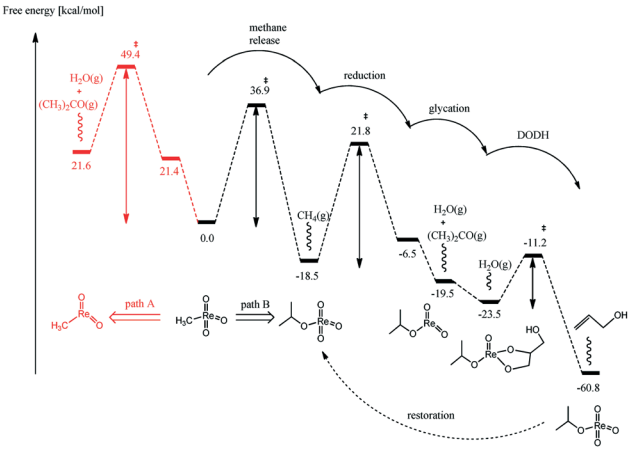

Scheme 4 Free energy profiles for the MTO reduction following path A and complete path B reaction routes.

(Scheme 4). Indeed, both ReO_2(2-PrO) glycation and subsequent DODH of the corresponding chelated product are strongly exergonic with the highest kinetic barrier of only 13 kcal mol^{-1}, *i.e.* for the DODH step, thus consistent with a fast process.

Further calculations were carried out to shed some light on the formation of the precipitate, in particular to identify a plausible assembly scheme for both Re^{VII} and Re^{V} alkoxide species. The formation of both Re^{VII} and Re^{V} dimer species assembled *via* alkoxide bridges and geometrically similar to those reported in reference[40] was corroborated by DFT calculations (ESI† Fig. S18). Two coordination modes of the alcohol feature these dinuclear complexes, with two η^1-coordinated 2-PrOH molecules on each metal center and two μ-coordinated alkoxides within the two metal atoms. DFT calculations indicated that Re^{VII} → Re^{V} reduction of the dimer occurs with an activation barrier and reaction free energy comparable to those calculated for the monomer complex (Fig. 4). Interestingly, the η^1-2-PrOH turned out to be more reactive than μ-2-PrO, *i.e.* the former activation barrier is about 7 kcal mol^{-1} lower, probably because the conversion of a bridging alkoxide to ketone has a destabilizing effect on

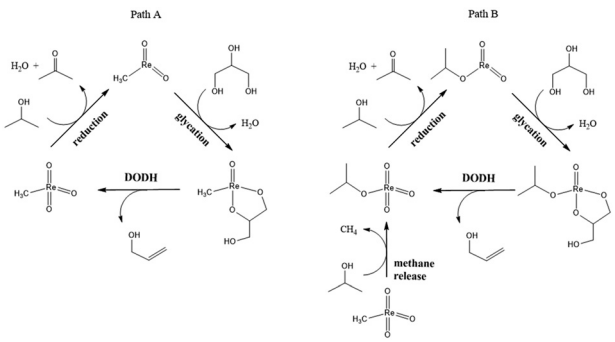

Scheme 3 Mechanism of the MTO catalysis of DODH of glycerol reported in the literature (path A, left),[24] and an alternative mechanism of MTO catalysis of DODH of glycerol including prior methane release (path B, right).

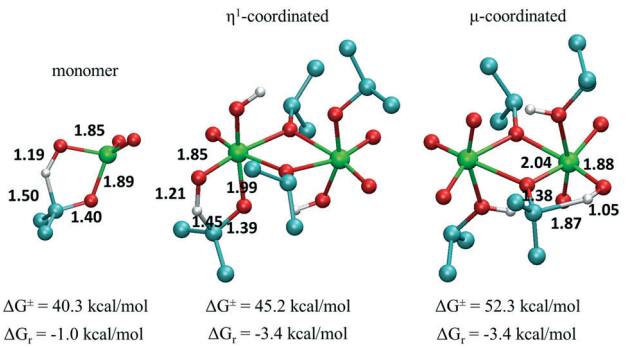

Fig. 4 Transition state structures for Re^{VII} → Re^{V} reduction occurring on mononuclear (left), and η^1-(middle) or μ-coordinated (right) dinuclear complexes. Distances in angstrom; activation ($\Delta G^{\pm}$) and reaction free energy (ΔG_r) are also reported.

the corresponding transition state structure. The higher reactivity of the η^1 ligands also suggests that $Re^{VII} \rightarrow Re^{V}$ reduction takes place mainly on the surface of the precipitate where bridging discontinuities are more likely. The calculated vibrational spectra of the dimer species were also found to disclose similarities with the experimental IR spectra collected for either **1** or **5** after a delay time (ESI† Table S1 and Fig. S19).

Discussion

An improved and possibly detailed elucidation of catalysis mechanisms is crucial for either the optimization or the scaling-up of a synthetic process, making it economically advantageous and industrially viable. Here, we have reported experimental and theoretical outcomes that could shed new light on the rhenium-catalysed DODH of glycerol operated in secondary alcohols.

The desired reaction product (AA) must be handled forced inside a cold trap since the reaction was conducted at temperatures noticeably higher than the boiling point of AA (97 °C). To facilitate this operation, a gas current is necessary and air represents a good choice as carrier gas even if the use of H_2 may increase the AA yield. Since it has been shown previously that H_2 does not act as the reducing agent,[15] its contribution consists in an increase in the reaction yield, mainly due to its inhibiting action towards the formation of by-products. In this regard, we have to clarify the origin of the by-products in the DODH reaction. On one hand, allyl formate, allyl acetate, and diallyl ether are secondary reaction products formed by the further reaction of allyl alcohol, whereas acrolein is formed through an independent pathway that starts directly from glycerol.[8c] Indeed, with the exception of acrolein (ESI† Table S2), all other by-products retrieved under an air current (*i.e.*, allyl formate, allyl acetate, diallyl ether *etc.*; ESI† Fig. S20), are totally absent under an H_2 current. This outcome corroborates the formation of acrolein through a completely different pathway compared to DODH, whereas the H_2 current probably contributes by inhibiting the further transformation of allyl alcohol into other derivatives that, if active, might contribute to a decrease in the final yields of AA.

In spite of their chemical diversity, we found mechanistic features shared by all the tested catalysts: i) the presence of a latency or delay time before detection of the product; ii) similar physical changes occurred in the reaction mixture, comprising formation of a precipitate. Our hypothesis is that operating at high temperature in a secondary alcohol, all the considered rhenium compounds undergo a similar mechanism of activation, leading to an active catalytic species. Indeed, experimental evidence indicates that the precipitate formed during the delay time corresponds to the same rhenium-species shown to catalyse the DODH of glycerol, independent of sourcing material. The IR analysis corroborated and provided further structural insights reinforcing this hypothesis. The narrow maximum around 920 cm^{-1} and the presence of signals within 2800–3500 cm^{-1} characterizing the precipitate was interpreted with the formation of Re^{VII} or another high oxidation state species assembled through the incorporation of alcohol moieties. These results may be explained by assuming that the DODH operating conditions promote under thermodynamic control the formation of rhenium alkoxide precipitates. The rhenium centres exposed to the bulk solvent may be thus considered the catalytic spots on which the further steps of the DODH process take place, *i.e.* reduction, glycation, and AA formation.

Special attention was then paid to compound **1**, *i.e.* MTO, whose importance in the catalysis of deoxygenation is widely recognized.[8b,c,13c,15] Based on previous outcomes, this complex not only undergoes latency and the formation of a precipitate in analogy to the other examined rhenium compounds, but it also releases methane during the delay time. Further experiments, performed in deuterated-DMP, showed the formation of CH_3D that indicates the participation of the solvent in the release process.[15] In the light of its importance in catalysis, the mechanism of methane release and catalytic activation of MTO was investigated in detail by means of DFT methods. Possible mechanisms for the MTO-catalysed DODH of glycerol have already been reported by the employment of quantum mechanical approaches.[24] Above all, the picture of MTO catalysis of DODH gained from these studies may be summarized in a three-step cyclic scheme comprising reduction, glycation, and re-oxidation of the Re centre,[24,39] corresponding to path A reported in Scheme 3.

On the other hand, the above-presented evidence motivated our DFT studies into the elucidation of a viable mechanistic alternative to path A including methane release in the initial steps of the process. Our calculations indicate that the release of methane from MTO occurs through a concerted mechanism in which the solvent donates a proton to the leaving CH_3^- during the cleavage of the Re–C bond. This step yields a Re^{VII} alkoxide species that we supposed to aggregate in the reaction conditions to form the precipitate. Analogous behaviour was previously described by Herrmann and Fischer who studied the polymerisation of MTO in aqueous solution.[37] They equally detected the production of methane with a concomitant formation of an oxo-rhenium oligomer featuring a methyl group content that was always lower than the starting MTO. Even the colour changes and the possible formation of dark solid residues are similar to our observations, strictly depending on the experimental conditions. The Re^{VII} centres on the surface of this solid material can then react through a Jones-like mechanism by yielding Re^{V} species that in turn correspond to catalytic spots on the precipitate surface. This mechanistic hypothesis basically comprises path B (Scheme 3), only differing in the nature of Re^{VII} and Re^{V} species as being part of a solid phase assembly (Scheme 5).

This mechanistic hypothesis is fairly corroborated by experimental outcomes like the formation of CH_3D in deuterated DMP[15] and the presence of IR signals ascribable to the alkoxide moiety in the IR spectra of **1** after a delay time.

A mechanistic hypothesis of the Re-catalysed DODH operating in secondary alcohol and at high temperatures can now

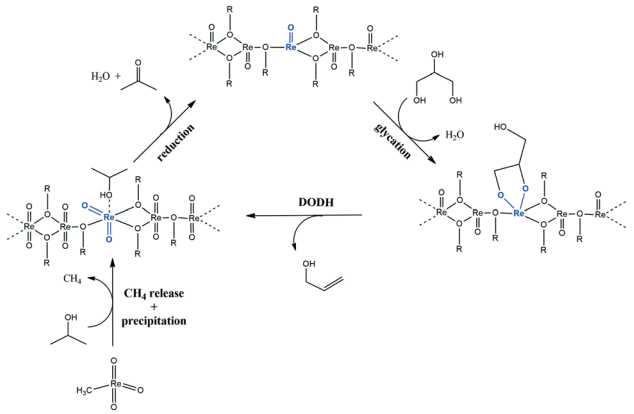

Scheme 5 A mechanistic hypothesis of MTO catalysis of DODH comprising methane release and formation of precipitate. *R* = 2,4-dimethyl-3-pentanyl. A catalytic spot is denoted in blue.

be drawn based on these outcomes. As exemplified by the computational analysis of MTO-catalysis in which methane release was found to be necessary to the activation of this catalyst, each starting rhenium material undergoes an activation process by reacting with the secondary alcohol to produce a precipitate. The rate of this initial process controls the duration of the delay time, depending on the particular chemistry involved. For example, ReO_3 may undergo disproportionation in the alcoholic phase, yielding both Re^{VII} and Re^{V} species, whereas ReI_3 would undergo solvolysis and oxidation, in both cases affording high-oxidation Re species. The described operating conditions herein seem to be able to operate on any Re material, rather independently of the starting oxidation state, to induce the formation of Re^{VII} alkoxide and its further precipitation. Indeed, XPS analyses clearly evidenced that the surface of the solid residues obtained from **1**, **4**, **5**, and **7** is mainly constituted by Re^{VII} and Re^{V}/Re^{IV}, the latter probably being formed by the reaction with the alcoholic solvent *via* the Jones-like reduction of Re^{VII} centres. Thus, the investigation herein reported indicated that the precipitate formed, above all, during the delay time, might be the actual catalyst of DODH, thus markedly changing our mechanistic view of the process by turning from homogeneous, as mostly reported in the literature, to heterogeneous catalysis, even if, with the coming of nanotechnologies, it always becoming more difficult to certainly define a catalytic process as merely homo- or merely heterogeneous. To support this innovative approach, we mention an interesting study undertaken by Anainikov and Beletskaya who have demonstrated that, at least in the cross-coupling reactions, the pathways involving soluble metal complexes and insoluble metal particles may take place at the same time, and both can contribute to the formation of the desired reaction product.[41]

Conclusions

AA was obtained in good yields in secondary alcohol solution and in the presence of different 1 mol% rhenium catalysts. In spite of their nature, all catalysts were transformed during a delay time into active species, solid in appearance, within a common process scheme that comprises the formation and aggregation of Re^{VII} alkoxide followed by Jones-like reduction to Re^{V}.

The specific case of MTO, *i.e.* compound **1**, is emblematic because of the release of methane coupled to the formation of Re^{VII} alkoxide under the considered reaction conditions. With the support of DFT calculations, a plausible mechanism for the activation of MTO catalysis was disclosed, including methane release. By taking together experimental and theoretical outcomes, a plausible mechanist hypothesis was drawn up, by which each starting Re material operated in alcohol and at high temperature produced, with variable delay times, a precipitate that in turn corresponded to the real catalyst for DODH. By shedding new light on rhenium-based catalysis, the results of the present investigation together with their interpretation could be of crucial importance in the future development of the DODH reaction and its role in glycerol valorisation.

Conflicts of interest

There are no conflicts to declare.

Acknowledgements

We are grateful to the "Consorzio per l'Innovazione Tecnologica, la Qualità e la Sicurezza degli Alimenti" (ITQSA) for financial support (CIPE DM 61318). A. M. and M. L. thank the "Ministero dell'Istruzione, dell'Università e della Ricerca" (MIUR) for the grants received for their PhD research program (Fondo Sostegno Giovani – FSG – 2012 and 2013; DM 10.12. 2013, no. 1016).

Notes and references

1 C. J. Li and P. T. Anastas, *Chem. Soc. Rev.*, 2012, **41**, 1413.
2 P. T. Anastas and J. C. Warner, in *Green Chemistry: Theory and Practice*, Oxford University Press, New York, 1998, p. 30.
3 (*a*) L. R. Lynd, X. Liang, M. J. Biddy, A. Allee, H. Cai, T. Foust, M. E. Himmel, M. S. Laser, M. Wang and C. E. Wyman, *Curr. Opin. Biotechnol.*, 2017, **45**, 202; (*b*) Q. Liu, S. C. Chmely and N. Abdoulmoumine, *Energy Fuels*, 2017, **31**, 3525; (*c*) S. Wang, G. Dai, H. Yang and Z. Luo, *Prog. Energy Combust. Sci.*, 2017, **62**, 33.
4 (*a*) P. Gallezot, *Chem. Soc. Rev.*, 2012, **41**, 1538; (*b*) C. O. Tuck, E. Pérez, I. T. Horváth, R. A. Sheldon and M. Poliakoff, *Science*, 2012, **337**, 695; (*c*) A. Corma, S. Iborra and A. Velty, *Chem. Rev.*, 2007, **107**, 2411.
5 (*a*) A. Pawelczyk, EU policy and legislation on recycling of organic wastes to agriculture, *ISAH*, 2005, **1**, 64; (*b*) C. Fritsch, A. Staebler, A. Happel, M. A. Cubero Márquez, I. Aguiló-Aguayo, M. Abadias, M. Gallur, I. M. Cigognini, A. Montanari, M. J. López, F. Suárez-Estrella, N. Brunton, E. Luengo, L. Sisti, M. Ferri and G. Belotti, *Sustainability*, 2017, **9**, 1492.

6 (*a*) C. Zhao, T. Brück and J. Lercher, *Green Chem.*, 2013, **15**, 1720; (*b*) R. A. Sheldon, *Green Chem.*, 2014, **16**, 950; (*c*) S. Dutta, *ChemSusChem*, 2012, **5**, 2125.

7 M. Lupacchini, A. Mascitti, G. Giachi, L. Tonucci, N. d'Alessandro, J. Martinez and E. Colacino, *Tetrahedron*, 2017, **73**, 609.

8 (*a*) S. Raju, M. E. Moret and R. J. M. Klein Gebbink, *ACS Catal.*, 2015, **5**, 281; (*b*) M. Shiramizu and F. D. Toste, *Angew. Chem., Int. Ed.*, 2012, **51**, 8082; (*c*) J. Yi, S. Liu and M. M. Abu-Omar, *ChemSusChem*, 2012, **5**, 1401; (*d*) C. Boucher-Jacobs and K. M. Nicholas, *ChemSusChem*, 2013, **6**, 597; (*e*) J. ten Dam and U. Hanefeld, *ChemSusChem*, 2011, **4**, 1017.

9 (*a*) G. Chapman and K. M. Nicholas, *Chem. Commun.*, 2013, **49**, 8199; (*b*) K. M. Kwok, C. K. S. Choong, D. S. W. Ong, J. C. Q. Ng, C. G. Gwie, L. Chen and A. Borgna, *ChemCatChem*, 2017, **9**, 2443; (*c*) A. Galindo, *Inorg. Chem.*, 2016, **55**, 2284; (*d*) A. R. Petersen, L. B. Nielsen, J. R. Dethlefsen and P. Fristrup, *ChemCatChem*, 2018, **10**, 769.

10 (*a*) J. R. Dethlefsen, D. Lupp, A. Teshome, L. B. Nielsen and P. Fristrup, *ACS Catal.*, 2015, **5**, 3638; (*b*) L. Hills, R. Moyano, F. Montilla, A. Pastor, A. Galindo, E. Álvarez, F. Marchetti and C. Pettinari, *Eur. J. Inorg. Chem.*, 2013, 3352; (*c*) L. Sandbrink, K. Beckerle, I. Meiners, R. Liffmann, K. Rahimi, J. Okuda and R. Palkovits, *ChemSusChem*, 2017, **10**, 1.

11 A. R. Petersen and P. Fristrup, *Chem. – Eur. J.*, 2017, **23**, 10235.

12 G. K. Cook and M. A. Andrews, *J. Am. Chem. Soc.*, 1996, **118**, 9448.

13 (*a*) V. Canale, R. Robinson Jr, A. Zavras, G. N. Khairallah, N. d'Alessandro, B. F. Yates and R. A. J. O'Hair, *J. Phys. Chem. Lett.*, 2016, **7**, 1934; (*b*) S. M. Bischof, M. J. Cheng, R. J. Nielsen, T. B. Gunnoe, W. A. Goddart III and R. A. Perriana, *Organometallics*, 2011, **30**, 2079; (*c*) R. G. Harms, W. A. Herrmann and F. E. Kühn, *Coord. Chem. Rev.*, 2015, **296**, 1.

14 (*a*) N. Ota, M. Tamura, Y. Nakagawa, K. Okumura and K. Tomishige, *Angew. Chem., Int. Ed.*, 2015, **54**, 1897; (*b*) J. Li, M. Lutz, M. Otte and R. J. M. Klein Gebbink, *ChemCatChem*, 2018, **10**, 4755; (*c*) Y. Nakagawa, S. Tazawa, T. Wang, M. Tamura, N. Hiyoshi, K. Okumura and K. Tomishige, *ACS Catal.*, 2018, **8**, 584.

15 V. Canale, L. Tonucci, M. Bressan and N. d'Alessandro, *Catal. Sci. Technol.*, 2014, **4**, 3697.

16 (*a*) A. L. Denning, H. Dang, Z. Liu, K. M. Nicholas and F. C. Jentoft, *ChemCatChem*, 2013, **5**, 3567; (*b*) J. Davis and R. S. Srivastava, *Tetrahedron Lett.*, 2014, **55**, 4178.

17 E. Arceo, J. A. Ellman and R. G. Bergman, *J. Am. Chem. Soc.*, 2010, **132**, 11408.

18 G. Sánchez, V. Gaikwad, C. Holdsworth, B. Dlugogorski, E. Kennedy and M. Stockenhuber, *Chem. Eng. J.*, 2016, **291**, 279.

19 B. T. Maru, F. López, S. W. M. Kengen, M. Constantí and F. Medina, *Fuel*, 2016, **186**, 375.

20 G. Bagnato, A. Iulianelli, A. Sanna and A. Basile, *Membranes*, 2017, **7**, 17.

21 M. Matsubara, N. Urano, S. Yamada, A. Narutaki, M. Fujii and M. J. Kataoka, *Biosci. Bioeng.*, 2016, **122**, 421.

22 M. Saini, Z. W. Wang, C. J. Chiang and J. P. Chao, *Biotechnol. Biofuels*, 2017, **10**, 173.

23 L. Harvey, E. Kennedy, B. Z. Dlugogorski and M. Stockenhuber, *Appl. Catal., A*, 2015, **489**, 241.

24 (*a*) X. Li, D. Wu, T. Lu, G. Yi, H. Su and Y. Zhang, *Angew. Chem., Int. Ed.*, 2014, **53**, 4200; (*b*) J. Shakeri, H. Hadadzadeh, H. Farrokhpour, M. Joshaghani and M. J. Weil, *J. Phys. Chem. A*, 2017, **121**, 8688; (*c*) S. Liu, A. Senocak, J. L. Smeltz, L. Yang, B. Wegenhart, J. Yi, H. Kenttämaa, E. Ison and M. M. Abu-Omar, *Organometallics*, 2013, **32**, 3210; (*d*) D. S. Morris, K. van Rees, M. Curcio, M. Cokoja, F. E. Kühn, F. Duarte and J. B. Love, *Catal. Sci. Technol.*, 2017, **7**, 5644; (*e*) P. Liu and K. M. Nicholas, *Organometallics*, 2013, **32**, 1821.

25 M. J. Frisch, G. W. Trucks, H. B. Schlegel, G. Scuseria, M. A. Robb, J. R. Cheeseman, G. Scalmani, V. Barone, B. Mennucci, G. A. Petersson, H. Nakatsuji, M. Caricato, X. Li, H. P. Hratchian, A. F. Izmaylov, J. Bloino, G. Zheng, J. L. Sonnenberg, M. Hada, M. Ehara, K. Toyota, R. Fukuda, J. Hasegawa, M. Ishida, T. Nakajima, Y. Honda, O. Kitao, H. Nakai, T. Vreven, J. A. Montgomery, Jr., J. E. Peralta, F. Ogliaro, M. Bearpark, J. J. Heyd, E. Brothers, K. N. Kudin, V. N. Staroverov, T. Keith, R. Kobayashi, J. Normand, K. Raghavachari, A. Rendell, J. C. Burant, S. S. Iyengar, J. Tomasi, M. Cossi, N. Rega, J. M. Millam, M. Klene, J. E. Knox, J. B. Cross, V. Bakken, C. Adamo, J. Jaramillo, R. Gomperts, R. E. Stratmann, O. Yazyev, A. J. Austin, R. Cammi, C. Pomelli, J. W. Ochterski, R. L. Martin, K. Morokuma, V. G. Zakrzewski, G. A. Voth, P. Salvador, J. J. Dannenberg, S. Dapprich, A. D. Daniels, O. Farkas, J. B. Foresman, J. V. Ortiz, J. Cioslowski and D. J. Fox, *Gaussian 09, Revision D.01*, Gaussian, Inc., Wallingford CT, 2013.

26 A. D. Becke, *J. Chem. Phys.*, 1993, **98**, 5648.

27 T. H. Dunning Jr. and P. J. Hay, in *Modern Theoretical Chemistry*, ed. H. F. Schaefer III, Plenum, New York, 1977, vol. 3, pp. 1–28.

28 (*a*) P. J. Hay and W. R. Wadt, *J. Chem. Phys.*, 1985, **82**, 270; (*b*) W. R. Wadt and P. J. Hay, *J. Chem. Phys.*, 1985, **82**, 284; (*c*) P. J. Hay and W. R. Wadt, *J. Chem. Phys.*, 1985, **82**, 299.

29 (*a*) R. Ditchfield, W. J. Hehre and J. A. Pople, *J. Chem. Phys.*, 1971, **54**, 724; (*b*) M. M. Francl, W. J. Pietro, W. J. Hehre, J. S. Binkley, D. J. DeFrees, J. A. Pople and M. S. Gordon, *J. Chem. Phys.*, 1982, **77**, 3654; (*c*) V. A. Rassolov, M. A. Ratner, J. A. Pople, P. C. Redfern and L. A. Curtiss, *J. Comput. Chem.*, 2001, **22**, 976.

30 A. D. McLean and G. S. Chandler, *J. Chem. Phys.*, 1980, **72**, 5639.

31 D. Andrae, U. Häussermann, M. Dolg, H. Stoll and H. Preuss, *Theor. Chim. Acta*, 1980, **77**, 123.

32 W. Küchle, M. Dolg, H. Stolland and H. Preuss, Pseudopotentials of the Stuttgart/Dresden group 1998, revision, August 11, 1998, http://www.theochem.uni-stuttgart.de/pseudopotentiale.

33 J. M. L. Martin and A. Sundermann, *J. Chem. Phys.*, 2001, **114**, 3408.

34 J. Tomasi, B. Mennucci and R. Cammi, *Chem. Rev.*, 2005, **105**, 2999.
35 Y. Kon, M. Araque, T. Nakashima, S. Paul, F. Dumeignil and B. Katryniok, *ChemistrySelect*, 2017, **2**, 9864.
36 A. Di Giuseppe, M. Crucianelli, M. Passacantando, S. Nisi and R. Saladino, *J. Catal.*, 2010, **276**, 412.
37 W. A. Herrmann and R. W. Fischer, *J. Am. Chem. Soc.*, 1995, **117**, 3223.
38 C. Boucher-Jacobs, P. Liu and K. M. Nicholas, *Organometallics*, 2018, **37**, 2468.
39 S. C. A. Sousa and A. C. Fernandes, *Coord. Chem. Rev.*, 2015, **284**, 67.
40 W. A. Herrmann, W. A. Wojtczak, G. R. J. Artus, F. E. Kühn and M. R. Mattner, *Inorg. Chem.*, 1997, **36**, 465.
41 V. P. Ananikov and I. P. Beletskaya, *Organometallics*, 2012, **31**, 1595.